A Riemann Solver for Wet/Dry Interfaces in Geoclaw

Dr. Brian KYANJO Prof. Donna CALHOUN

Department of Mathematics
Boise State University

September 21st, 2021

Outline

Riemann Problem

A Riemann Problem is a fundamental problem in conservation laws and is useful in finite volume schemes.

$$q_t + f(q)_x = 0 \tag{1}$$

$$q(x,0) = \begin{cases} q_L, & \text{if } x \leq 0, \\ q_R, & \text{if } x > 0, \end{cases} \tag{2}$$

where $f(q)_x \in \mathbb{R}^m$ is a vector of conserved quantities, q_R and q_L are two piece-wise constant states separated by a discontinuity.

Shallow Water Equations (SWE)

The SWE are a system of hyperbolic PDEs governing the flow below a pressure surface in a fluid.

$$\begin{aligned} h_t + (uh)_x &= 0 \\ (hu)_t + \left(hu^2 + \frac{1}{2}\rho g h^2 \right)_x &= 0 \end{aligned} \tag{3}$$

where $h(x,t)$ depicts the the height field, hu measures the flow rate of water past a point, ρ (kg/m^3) is the constant density of the incompressible fluid, and $u(x,t)$ (m/s) is the horizontal velocity. We will set $\rho = 1$ here.[3].

Cont.

A very simple set of initial conditions is a single discontinuity at the middle of the channel.
At $x = 0$ and $t = 0$, the discontinuity is located between the left and right state, so the solution at the left (q_l)and right(q_r) states are given by:

$$q_l = \begin{bmatrix} h_l \\ (hu)_l \end{bmatrix} \quad \text{and} \quad q_r = \begin{bmatrix} h_r \\ (hu)_r \end{bmatrix} \tag{4}$$

The variation of h and hu on either side of the discontinuity leads the waves in the Riemann problem to move at different speeds creating discontinuities (shocks) or changing regions (rarefactions).

Regions

As t increases, four distinct regions are created, separated by characteristics. The middle state called the intermediate state(q_m), is generated. The determination of this state characterizes the Riemann problem and how it connects to other states via waves in each respective characteristic family[1].

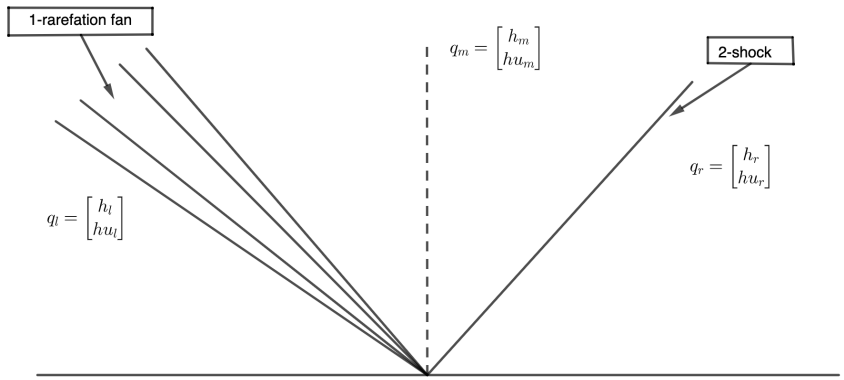

Figure: x-t plane showing the connection of states, 1-rarefaction fan, and the 2-shock.

Exact Riemann Solver

The shock speed, $s(t)$, from the shock wave as the solution emerges is determined from the Rankine-Hugoniot jump condition given by equation (5) which must be satisfied across any shock wave.
If q_l and q_r are connected by a shock, the Rankine Hugoniot conditions will be satisfied.

$$\begin{aligned} s_1(q_m - q_l) &= f(q_m) - f(q_l) \\ s_2(q_r - q_m) &= f(q_r) - f(q_m) \end{aligned} \tag{5}$$

By applying condition (5) to shallow water equations (3) creates a system of four equations (6) that must be satisfied simultaneously.

Cont.

$$
\begin{aligned}
s_1(h_m - h_l) &= hu_m - hu_l \\
s_1(hu_m - hu_l) &= hu_m^2 - hu_l^2 + \frac{1}{2}g(h_m^2 - h_l^2) \\
s_2(h_r - h_m) &= hu_r - hu_m \\
s_1(hu_r - hu_m) &= hu_r^2 - hu_m^2 + \frac{1}{2}g(h_r^2 - h_m^2)
\end{aligned}
\tag{6}
$$

Since the (h_l, u_l) and (h_r, u_r) are fixed, we find all states: (h_m, u_m) and their corresponding speeds: s_1 and s_2 that satisfy system (6).
We have four equations and four unknowns, which gives a two parameter family of solutions: one-shock and two-shock.

Hugoint Loci

Using h_l and h_r as parameters, corresponding u_l, u_r, s_1,and s_2 are determined for each h_l and h_r. And then a graph of hu against h.

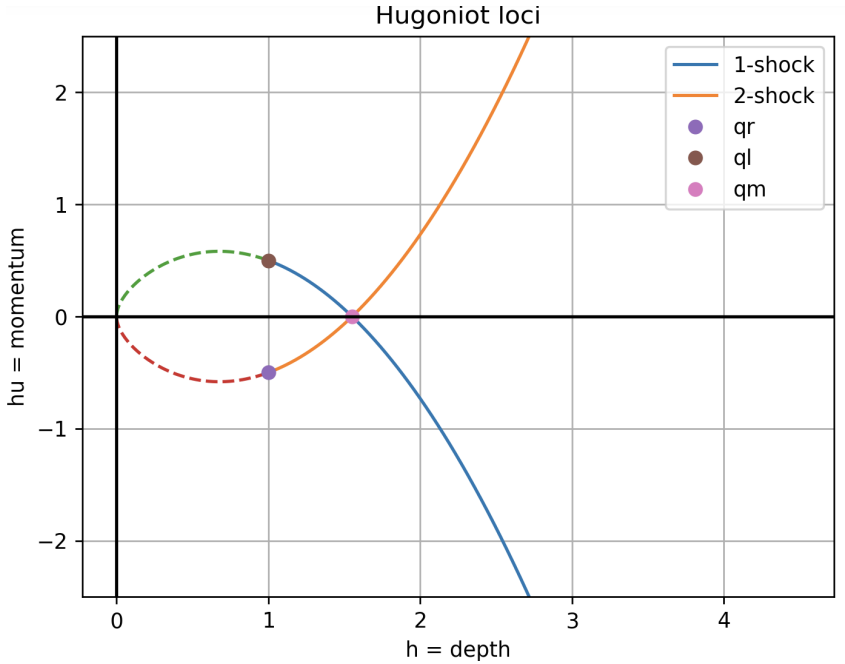

Figure: Shows curves that represent all states connected to q_l and all states connected to q_r via a *2-shock* and *1-shock* respectively.

Non-linear Equation

The point q_m lies on the curve (7) of points through point q_r that connects to q_r by a *2-shock*.

$$u_m = u_r + (h_m - h_r)\sqrt{\frac{g}{2}\left(\frac{1}{h_m} + \frac{1}{h_r}\right)} \tag{7}$$

Likewise, the state(q_m), must also lie on the Hugonoit locus (equation (8)) of the 1-shock wave passing through q_l

$$u_m = u_l - (h_m - h_l)\sqrt{\frac{g}{2}\left(\frac{1}{h_m} + \frac{1}{h_l}\right)} \tag{8}$$

Example

Consider athe SWE Riemann problem with $h_l = h_r = 1, u_l = 0.5$, and $u_r = -0.5$. These initial values are used by the netwon solver to solve equations (7) and (8) to produce $h_{ms} = 1.554$

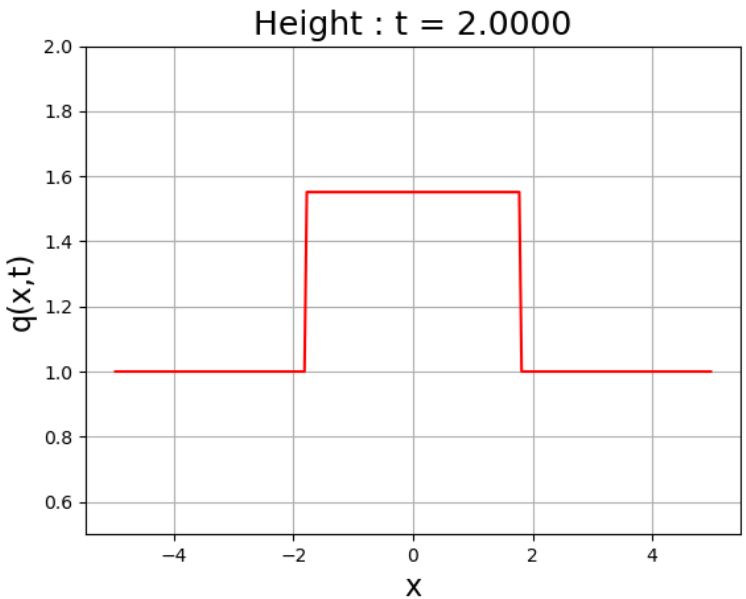

Figure: Shows all-shock Riemann exact solution

```
for i in range(len(x)):
    if 0.5*(sl(hl,ql,g) + sl(hms,qms,g))*t > x[i] :
            h = hl
            u = ul
            hu = h*u
    elif sl(hms,qms,g)*t < x[i] and x[i]<t*sr(hms,qr,g
    ):
            h = hms
            u = ums
            hu = h*u
    else:
            h = hr
            u = ur
            hu = h*u
    q1[i] = h
    q2[i] = hu
```

Listing 1: Python code describing how the two shock case solution is obtained after the first time step.

Finite Volume method (FVM

Consider a one dimensional (1D) conservation law (equation (9)), where q is the measure of conserved quantity density and $f(q)$ is a flux function.

$$q_t(x,t) + f(q(x,t))_x = 0 \tag{9}$$

Consider $C_i = (x_{i-\frac{1}{2}}, x_{i+\frac{1}{2}})$ to be the i^{th} grid cell, the average value over the i^{th} interval at time t^n is numerically approximated by Q_i^n in equation (16).

$$Q_i^n \approx \frac{1}{\Delta x} \int_{C_i} q(x,t^n)dx \tag{10}$$

where $\Delta t = (t^{n+1} - t^n)$ and $\Delta x = (x_{i+\frac{1}{2}} - x_{i-\frac{1}{2}})$ is the cell length.

Cont.

A discontinuity in q violates the PDE in the classical sense and only holds for the integral conservation law (fundamental equation (11)).

$$\frac{d}{dt}\int_{c_i} q(x,t)dx = f(q(x_{i-\frac{1}{2}},t)) - f(q(x_{i+\frac{1}{2}},t)) \tag{11}$$

The approximate total integral of q over each grid cell is evaluated and updated at every time step by the grid cell edge fluxes.

$$Q_i^{n+1} = Q_i^n - \frac{\Delta t}{\Delta x}(F^n_{i+\frac{1}{2}} - F^n_{i-\frac{1}{2}}) \tag{12}$$

where $F^n_{i+\frac{1}{2}}$ is the average flux approximation along $x = x_{i-\frac{1}{2}}$.

Godnuv Approach.

Taking two neighbouring grid cells: $Q_{i-1} = q_L$ and $Q_i = q_R$ to be cell averages, this information is used by the exact Riemann solver to compute numerical fluxes ($F^n_{i-\frac{1}{2}} = \mathcal{F}(Q_{i-1}, Q_i)$), that are used to update the cell average at each time step [1]. Then equation (12) becomes:

$$Q_i^{n+1} = Q_i^n - \frac{\Delta t}{\Delta x}\left[\mathcal{F}(Q_i, Q_{i+1}) - \mathcal{F}(Q_{i-1}, Q_i)\right] \tag{13}$$

where $\mathcal{F}$ is some numerical flux function.

Wave Propagation Algorithm (WPA)

Equation (12), can be reformulated as a first order wave propagation method by decomposing flux at the cell averages into fluctuations ($\mathcal{A}^+\Delta Q^n_{i-\frac{1}{2}}$ and $\mathcal{A}^- Q^n_{i+\frac{1}{2}}$):

$$\mathcal{A}^+\Delta Q^n_{i-\frac{1}{2}} = f(Q_i) - f(Q^*_{i-\frac{1}{2}}) \tag{14}$$

$$\mathcal{A}^-\Delta Q^n_{i+\frac{1}{2}} = f(Q^*_{i+\frac{1}{2}}) - f(Q_i) \tag{15}$$

where $\mathcal{A}^+\Delta Q^n_{i-\frac{1}{2}}$ and $\mathcal{A}^- Q^n_{i+\frac{1}{2}}$ are the net updating contributions from the rightward and leftward moving waves into the grid cell C_i from the right and left interface respectively. Combining equations (14) and (15), the first order 1D wave propagation method is defined by:

$$Q^{n+1}_i = Q^n_i - \frac{\Delta t}{\Delta x}(\mathcal{A}^+\Delta Q^n_{i-\frac{1}{2}} + \mathcal{A}^- Q^n_{i+\frac{1}{2}}) \tag{16}$$

Wave Propagation Algorithm (WPA)

Equation (12), can be reformulated as a first order wave propagation method by decomposing flux at the cell averages into fluctuations ($\mathcal{A}^+\Delta Q^n_{i-\frac{1}{2}}$ and $\mathcal{A}^- Q^n_{i+\frac{1}{2}}$):

$$\mathcal{A}^+\Delta Q^n_{i-\frac{1}{2}} = f(Q_i) - f(Q^*_{i-\frac{1}{2}}) \tag{14}$$

$$\mathcal{A}^-\Delta Q^n_{i+\frac{1}{2}} = f(Q^*_{i+\frac{1}{2}}) - f(Q_i) \tag{15}$$

where $\mathcal{A}^+\Delta Q^n_{i-\frac{1}{2}}$ and $\mathcal{A}^- Q^n_{i+\frac{1}{2}}$ are the net updating contributions from the rightward and leftward moving waves into the grid cell C_i from the right and left interface respectively. Combining equations (14) and (15), the first order 1D wave propagation method is defined by:

$$Q^{n+1}_i = Q^n_i - \frac{\Delta t}{\Delta x}(\mathcal{A}^+\Delta Q^n_{i-\frac{1}{2}} + \mathcal{A}^- Q^n_{i+\frac{1}{2}}) \tag{16}$$

Quasi-linear form

The general conservation law in (9) can be written in *quasi-linear form* as

$$q_t + f'(q)q_x = 0 \tag{17}$$

where $f'(q) \in \mathbb{R}^{m \times m}$ flux Jacobian matrix. Consider a Riemann problem for the system (17) with initial data

$$q(x, t^n) = \begin{cases} Q_{i-1}^n & \text{if} \quad x < x_{i-\frac{1}{2}} \\ Q_i^n & \text{if} \quad x > x_{i-\frac{1}{2}} \end{cases} \tag{18}$$

The initial data is used by the exact Riemann solver to generate $q_m = (h_m, hu_m)$ which is used to evaluate the eigenvalues $(\lambda_{i-1/2})$ and eigenvectors $(r_{i-1/2})$ at $x = x_{i-\frac{1}{2}}$.

Cont.

Waves and speeds are obtained as an eigenvector decomposition of the jump in Q_i at the interface $i - \frac{1}{2}$. This decomposition takes the form

$$Q_i - Q_{i-1} = \sum_{p=1}^{m} \alpha_{i-\frac{1}{2}} r_{i-\frac{1}{2}} \tag{19}$$

The wave speed $s^p_{i-\frac{1}{2}}$ associated with the vector $r^p_{i-\frac{1}{2}}$, are preselected basing on the characteristic structure of the initial Riemann data [3].

Cont.

Therefore the fluctuations $\mathcal{A}^+\Delta Q^n_{i-\frac{1}{2}}$ and $\mathcal{A}^-\Delta Q^n_{i-\frac{1}{2}}$ are defined by equations (20) and (21):

$$\mathcal{A}^-\Delta Q^n_{i-\frac{1}{2}} = \sum_{\{p:s^p_{i-\frac{1}{2}}<0\}} s^p_{i-\frac{1}{2}} \mathcal{W}^p_{i-\frac{1}{2}} \tag{20}$$

$$\mathcal{A}^+\Delta Q^n_{i-\frac{1}{2}} = \sum_{\{p:s^p_{i-\frac{1}{2}}>0\}} s^p_{i-\frac{1}{2}} \mathcal{W}^p_{i-\frac{1}{2}} \tag{21}$$

In a standard conservative case ((9)), the sum of the left-going and right-going fluctuations should satisfy:

$$\mathcal{A}^+\Delta Q^n_{i-\frac{1}{2}} + \mathcal{A}^- Q^n_{i+\frac{1}{2}} = f(Q_i) - f(Q_{i-1}) \tag{22}$$

Second Order Accuracy

The second order accuracy is obtained by taking the correction terms into account as shown described in equation (23)

$$Q_i^{n+1} = Q_i^n - \frac{\Delta t}{\Delta x}(\mathcal{A}^+ \Delta Q^n_{i-\frac{1}{2}} + \mathcal{A}^- Q^n_{i+\frac{1}{2}}) - \frac{\Delta t}{\Delta x}(\tilde{F}^n_{i+\frac{1}{2}} - \tilde{F}^n_{i-\frac{1}{2}}) \quad (23)$$

where $\tilde{F}^n_{i-\frac{1}{2}}$ are second order correction terms determined by the waves and speeds in the Riemann problems after approximating the average flux along $x = x_{i-\frac{1}{2}}$:

$$\tilde{F}^n_{i-\frac{1}{2}} = \frac{1}{2}\sum_{p=1}^{m} |s^p_{i-\frac{1}{2}}| \left(1 - \frac{\Delta t}{\Delta x}|s^p_{i-\frac{1}{2}}|\right) \tilde{\mathcal{W}}^p_{i-\frac{1}{2}} \quad (24)$$

WPA for SWE

The combination of equations in system (3), forms a system of one-dimensional SWEs given by equation (25)

$$\begin{bmatrix} h \\ hu \end{bmatrix}_t + \begin{bmatrix} uh \\ hu^2 + \frac{1}{2}gh^2 \end{bmatrix}_x = 0 \tag{25}$$

Equation (25) can be written as a quasi-linear system as shown in equation (26):

$$\begin{bmatrix} h \\ hu \end{bmatrix}_t + \begin{bmatrix} 0 & 1 \\ -u^2 + gh & 2u \end{bmatrix} \begin{bmatrix} h \\ hu \end{bmatrix}_x = \begin{bmatrix} 0 \\ 0 \end{bmatrix} \tag{26}$$

where the flux Jacobian matrix $f'(q)$ is given by

$$f'(q) = \begin{bmatrix} 0 & 1 \\ -u^2 + gh & 2u \end{bmatrix} \tag{27}$$

Roe Solver

The non linear problem (equation (9)), can be replaced by a linearized problem defined locally at each cell interface,

$$\hat{q}_t + \hat{A}_{i-\frac{1}{2}} \hat{q}_x = 0 \tag{28}$$

where 2×2 matrix $\hat{A}_{i-\frac{1}{2}}$ (equation (29)) is selected to be an approximation of $f'(q)$ that is valid in the neighbourhood of the intial data Q_{i-1} and Q_i.

$$\hat{A}_{i-\frac{1}{2}} = \begin{bmatrix} 0 & 1 \\ -\hat{u}^2 + g\bar{h} & 2\hat{u} \end{bmatrix} \tag{29}$$

where $\bar{h} = \frac{1}{2}(h_{i-1} + h_i)$ is the average between end points h_{i-1} and h_i, g is the acceleration due to gravity, and $\hat{u} = (\sqrt{h_{i-1}}u_{i-1} + \sqrt{h_i}u_i)/(\sqrt{h_{i-1}} + \sqrt{h_i})$ is the Roe average.

Cont.

Since $\hat{A}_{i-\frac{1}{2}}$ is a real diagonalizable Jacobian matrix evaluated at $\hat{q} = (\bar{h}, \bar{h}\hat{u})$, then its eigenvalues ($\hat{\lambda}$) and eigenvectors ($\hat{r}$) are given by [**?**]:

$$\hat{\lambda}^1 = \hat{u} - \hat{c}, \qquad \hat{\lambda}^2 = \hat{u} + \hat{c} \tag{30}$$

$$\hat{r}^1 = \begin{bmatrix} 1 \\ \hat{\lambda}^1 \end{bmatrix}, \qquad \hat{r}^2 = \begin{bmatrix} 1 \\ \hat{\lambda}^2 \end{bmatrix} \tag{31}$$

where $\hat{c} = \sqrt{gh}$, The approximate Riemann solver is used to decompose the vector $\delta \equiv Q_i - Q_{i-1}$ into two waves: $\alpha^1_{i-\frac{1}{2}}\hat{r}^1$ and $\alpha^1_{i-\frac{1}{2}}\hat{r}^2$ as

$$Q_i - Q_{i-1} = \alpha^1_{i-\frac{1}{2}}\hat{r}^1 + \alpha^1_{i-\frac{1}{2}}\hat{r}^2 \equiv \mathcal{W}^1_{i-\frac{1}{2}} + \mathcal{W}^2_{i-\frac{1}{2}} \tag{32}$$

where the coefficients $\alpha^1_{i-\frac{1}{2}}$ are given by:

$$\alpha^1_{i-\frac{1}{2}} = \frac{(\hat{u}+\hat{c})\delta^1 - \delta^2}{2\hat{c}} \tag{33}$$

$$\alpha^2_{i-\frac{1}{2}} = \frac{-(\hat{u}-\hat{c})\delta^1 + \delta^2}{2\hat{c}} \tag{34}$$

Limiters: Accuracy of smooth solutions are obtained by advancing first order methods to second order accurate, but these still fail at the neighbourhood of discontinuities, where oscillations (noise) are created as shown in fig. 4b.

Numerical Examples

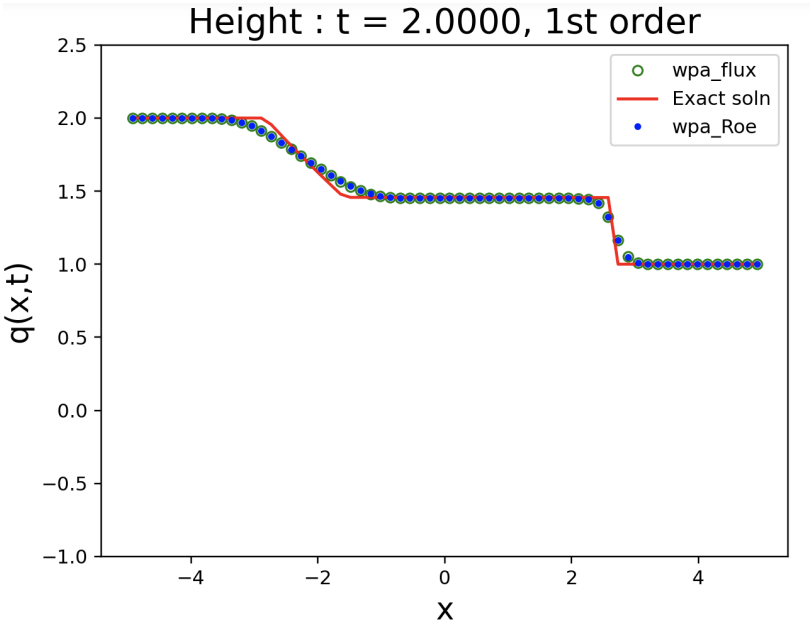

(a)

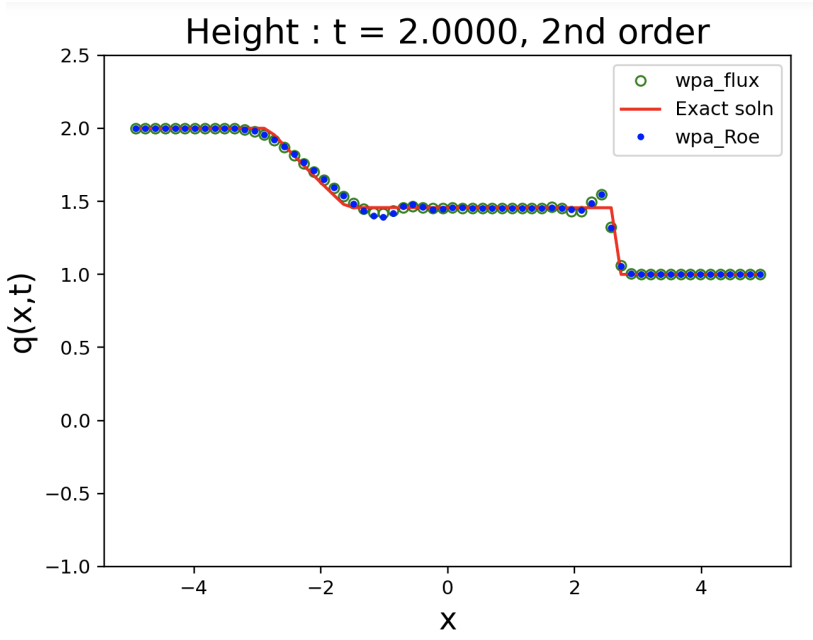

(b)

Figure: (a) and (b) respectively show height field at the final time step for both first and second order correction without limiters using 64 space points.

With limiters

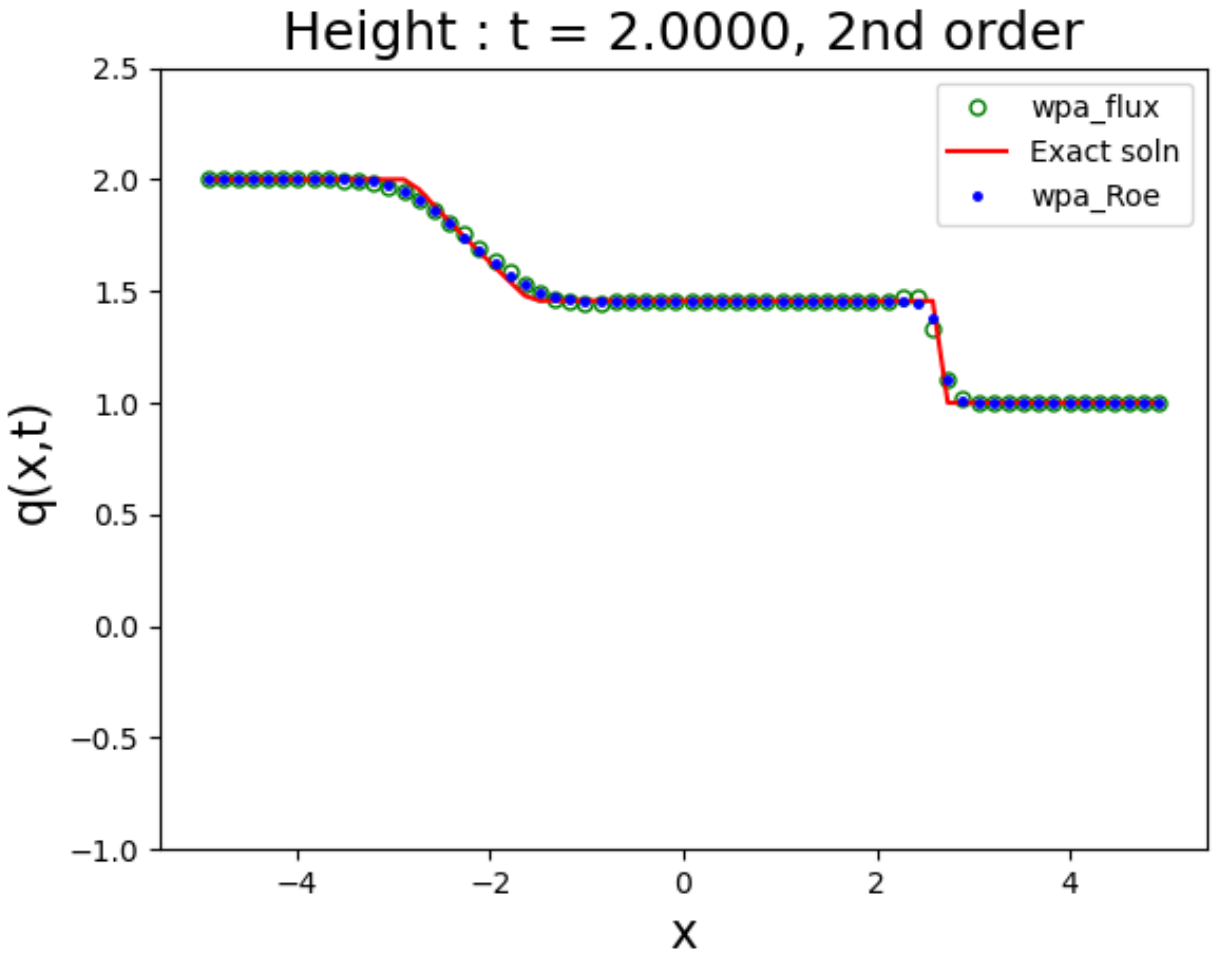

Figure: Shows the height field at the final time step of second order correction with limiter using 64 space points.

Bathymetric source terms

Equation (3), can be extended to balance equations by introducing a bathymetric source term as shown in equation (35). This is done by discretising the source term to generate values $-gh_{i-\frac{1}{2}}B'(x_{i-\frac{1}{2}})$ at cell interfaces $x = x_{i-\frac{1}{2}}$ [2].

$$\begin{aligned} h_t + (uh)_x &= 0 \\ (hu)_t + \left(hu^2 + \frac{1}{2}gh^2\right)_x &= -ghB'(x) \end{aligned} \tag{35}$$

where $B(x)$ represents bottom elevation.

F-wave Approach

The flux difference $f(Q_i) - f(Q_{i-1})$ is directly decomposed as a linear combination of the eigenvectors $r_{i-\frac{1}{2}}$ as shown in equation (36)

$$f(Q_i) - f(Q_{i-1}) - \Delta x \psi_{i-\frac{1}{2}} = \sum_{p=1}^{m} \beta^p_{i-\frac{1}{2}} r^p_{i-\frac{1}{2}} \equiv \sum_{p=1}^{m} \mathcal{Z}^p_{i-\frac{1}{2}} \tag{36}$$

where

$$\beta_{i-\frac{1}{2}} = R^{-1}_{i-\frac{1}{2}} \left(f(Q_i) - f(Q_{i-1})\right) - \Delta x \psi_{i-\frac{1}{2}} \tag{37}$$

The standard WPA first and second order corrections have been advanced to capture the flux based wave decomposition.

$$\tilde{F}^n_{i-\frac{1}{2}} = \frac{1}{2} \sum_{p=1}^{m} \text{sgn}(s^p_{i-\frac{1}{2}}) \left(1 - \frac{\Delta t}{\Delta x} |s^p_{i-\frac{1}{2}}|\right) \tilde{\mathcal{Z}}^p_{i-\frac{1}{2}} \tag{38}$$

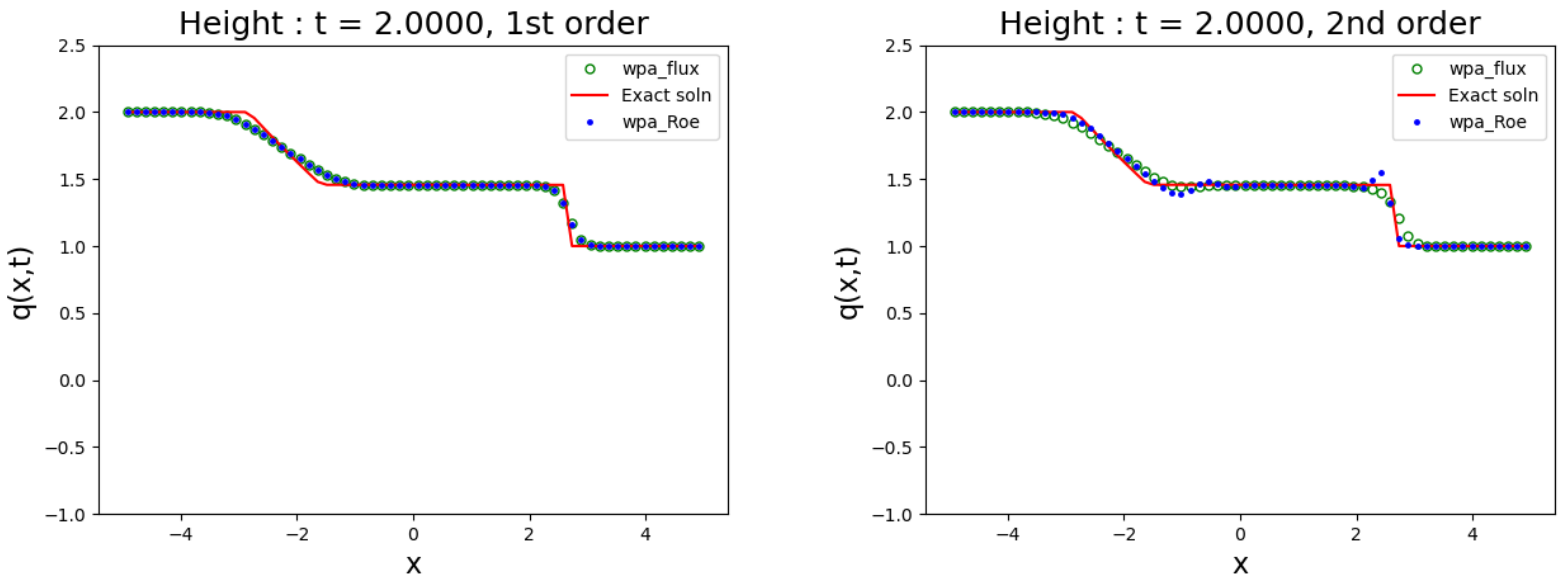

(a) (b)

Figure: (a) and (b) respectively show height field at the final time step for both first and second order correction without limiters obtained after introducing the source term and the f-wave method.

with Limiters

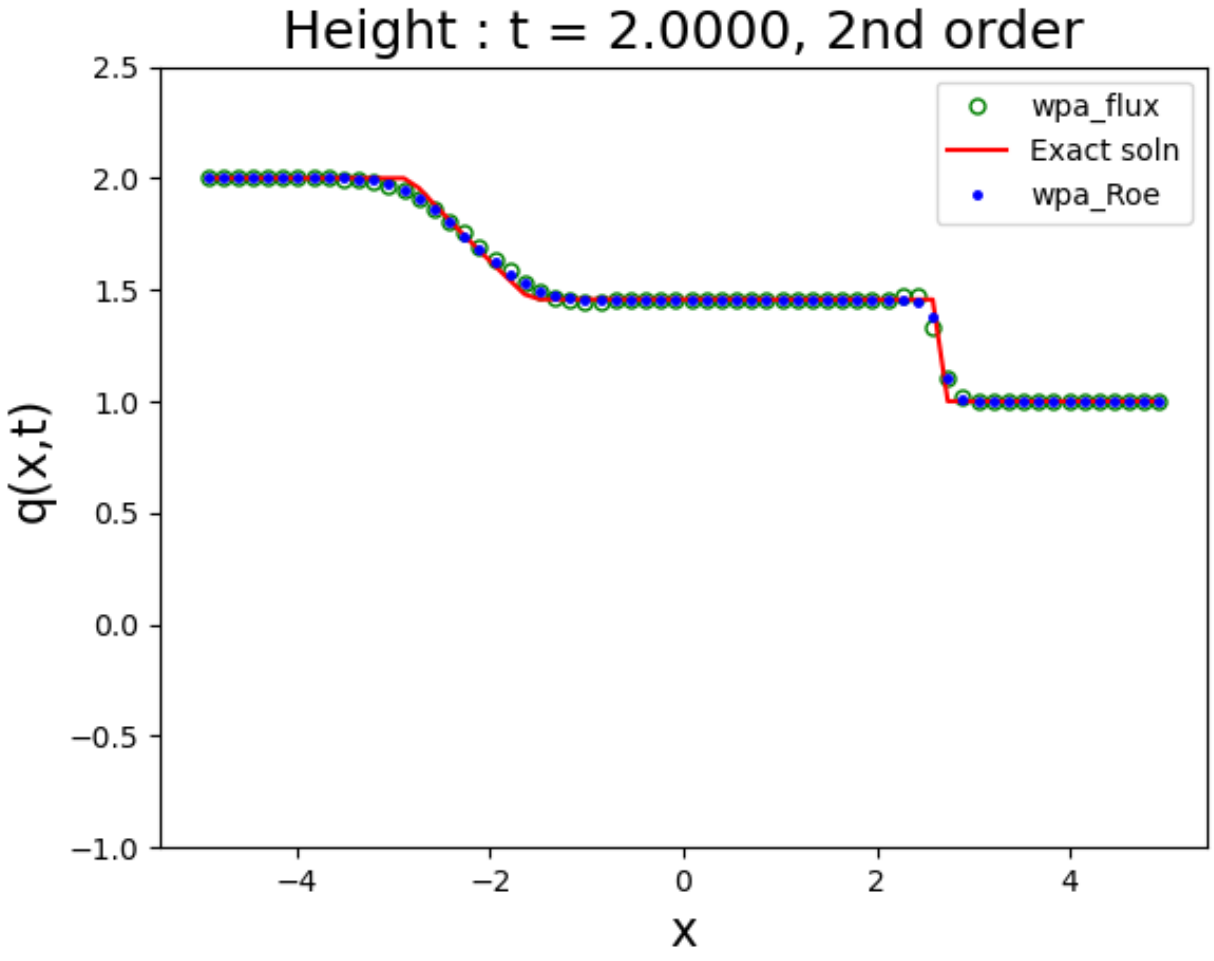

Figure: Shows the height field at the final time step of second order correction with limiter obtained after introducing the source term and the f-wave method using 64 space points.

Riemann Problem for Wet/Dry States

Dry states are regions with zero water depth [4]. In such states SWEs are not applicable, so we consider wet states adjacent to dry regions as shown in figure 12.

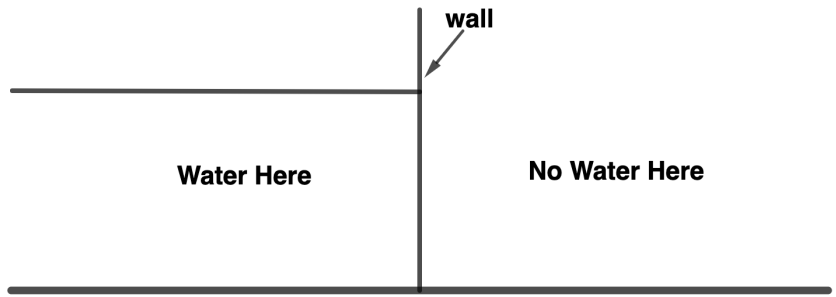

Figure: The Riemann problem with a dry bed (has no water) in one of the data state.

Three Possible cases

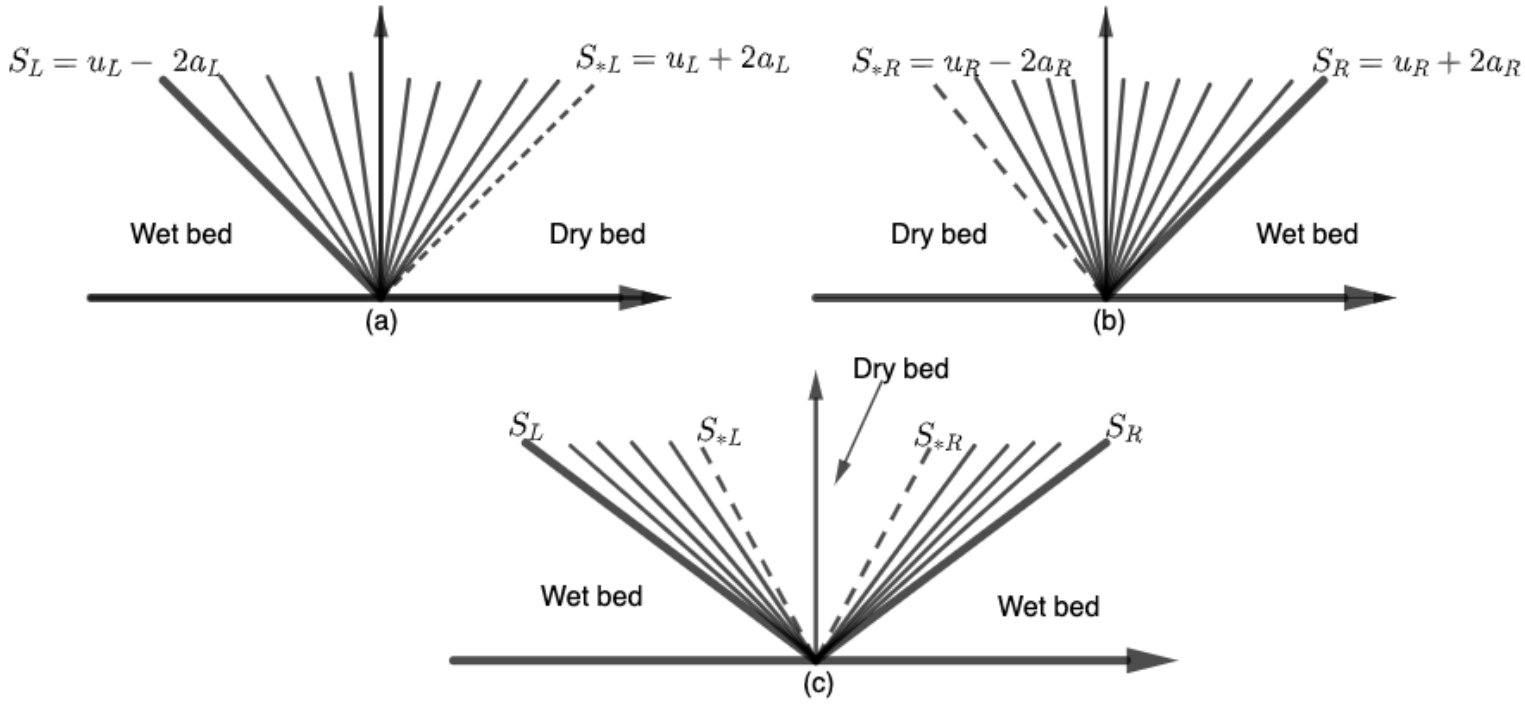

Figure: The dry state appears in three cases: (a) dry region is on the right, (b) dry region is on the left, and (c) dry region appears in the interaction of two wet bed states.

Right dry bed profile

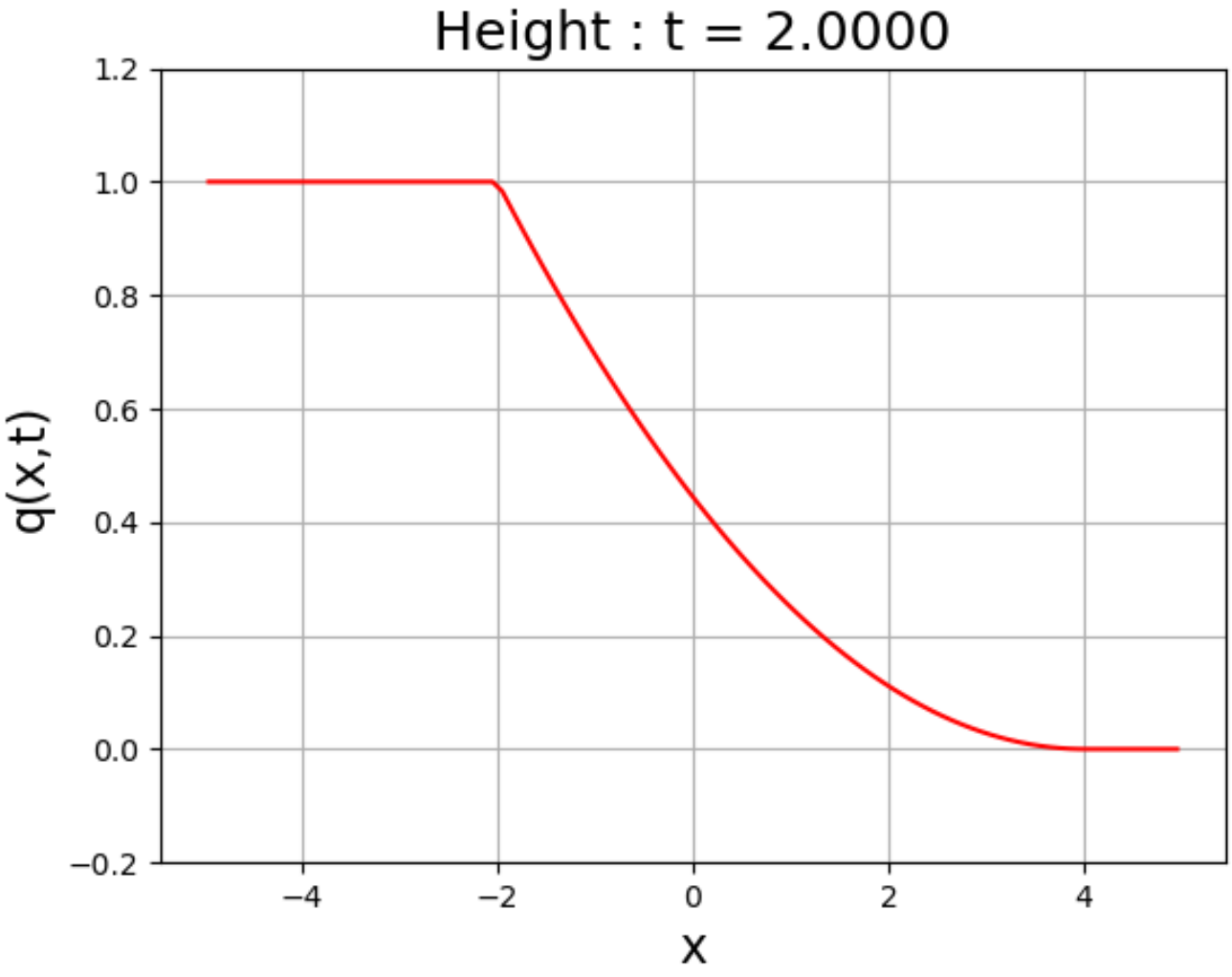

Figure: Shows a typical solution profile for the Riemann solution in which the dry bed is at the right

Left dry bed profile

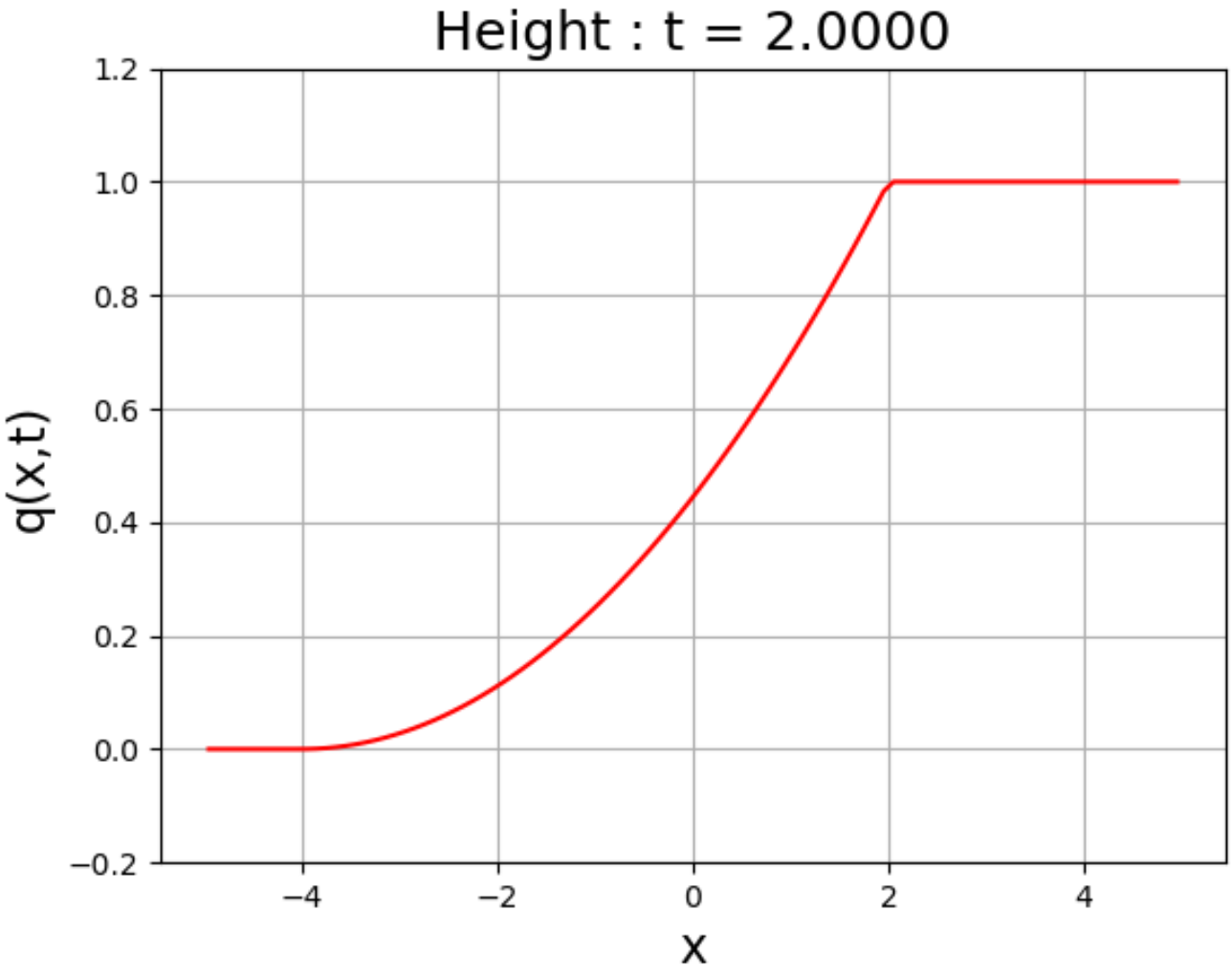

Figure: Shows a typical solution profile for the Riemann solution in which the dry bed is at the left

Middle dry bed profile

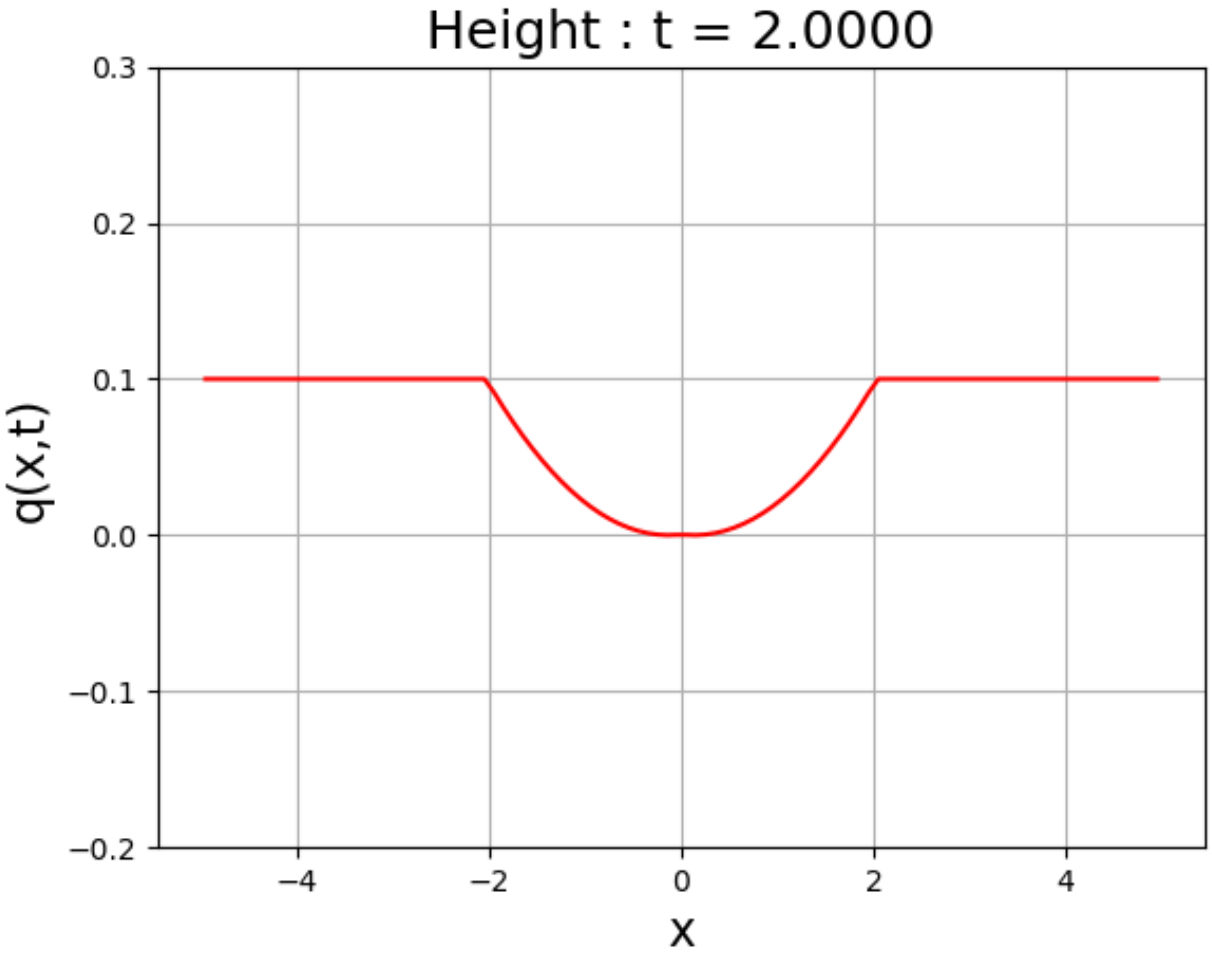

Figure: Shows a typical solution profile for the Riemann solution in which the dry bed appears in the interaction between the two wet bed regions.

Thank you!

briankyanjo@u.boisestate.edu

References

[1] Derek Bale, Randall J. LeVeque, Sorin Mitran, and James Rossmanith. A Wave Propagation Method for Conservation Laws and Balance Laws with Spatially Varying Flux Functions. 24(3):955–978, 2003.

[2] D. L. George. Adaptive finite volume methods with well-balanced Riemann solvers for modeling floods in rugged terrain: Application to the Malpasset dam-break flood (France, 1959). 66(8):1000–1018, 2011.

[3] David L. George. Augmented Riemann solvers for the shallow water equations over variable topography with steady states and inundation. 227(6):3089 – 3113, 2008.

[4] Randall J. LeVeque, David L. George, and Marsha J. Berger. Tsunami modelling with adaptively refined finite volume methods. 20:211 – 289, May 2011.